ACS Photonics

Article

pubs.acs.org/journal/apchd5

Multipolar Fano Resonances and Fano-Assisted Optical Activity in Silver Nanorice Heterodimers

Xiaorui Tian,[†] Yurui Fang,*[,‡] and Baile Zhang*[,†,§]

[†]Division of Physics and Applied Physics, School of Physical and Mathematical Sciences, and [§]Centre for Disruptive Photonic Technologies, Nanyang Technological University, 21 Nanyang Link, 637371, Singapore

[‡]Division of Bionanophotonics, Department of Applied Physics, Chalmers University of Technology, Göteborg SE-412 96, Sweden

Supporting Information

ABSTRACT: We propose a simple structure of a silver nanorice heterodimer to achieve both Fano resonances and strong optical activity. Due to the ellipsoid shape of nanorice, the dimer shows a unique plasmon hybridization picture, being different from those in previously studied two-nanoparticle coupling, which benefits the generation of Fano resonances here. Under oblique incidence, this nanorice dimer exhibits not only multipolar Fano resonances but also very strong optical activity in the Fano resonant ranges. A chiral molecule model is proposed to explain the generation of chirality. It is also shown that Fano resonance has an assisting effect on optical activity (especially for subradiant modes), which can be ascribed to the energy transfer from the super-radiant modes to the subradiant modes during Fano interference.

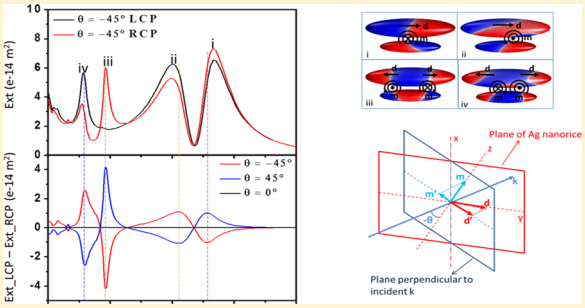

KEYWORDS: *nanorice heterodimer, multipolar Fano resonances, higher-order modes, chirality, optical activity*

Noble metal nanostructures possess many unique optical properties because of collective oscillations of electrons confined to metal−dielectric interfaces, known as surface plasmons (SPs),[1] which have numerous applications in various areas such as surface-enhanced spectroscopies,[2−5] subwavelength waveguiding,[6−10] and photocatalysis.[11] The plasmonic properties of a nanostructure are closely related to its shape, size, and the surrounding environment. When two or more nanostructures are placed next to each other, strong coupling through near-field interactions can give rise to a new set of hybridized plasmonic modes.[12,13] Plasmon hybridization of complex metal nanostructures offers a powerful strategy to tailor the spectral response of plasmons and then enable applications in nanoruler,[14,15] plasmonic circular dichroism (CD),[16] and sensing.[17,18]

Plasmonic Fano resonance, which arises from interference between spectrally overlapping narrow subradiant (dark) and broad super-radiant (bright) plasmonic modes, is a peculiar consequence of electromagnetic (EM) coupling in complex nanostructures. Due to its highly sensitive feature, Fano resonance has promising applications in biochemical sensing and has attracted tremendous interest recently.[19−21] In addition, Fano resonance has been used to enhance Raman signals and nonlinear optical processes.[22−24] Until now plasmonic resonances with a Fano-like line shape have been reported in quite a few metallic nanostructure systems.[19] Recently, higher-order Fano resonances, which are expected to have higher sensitivity, have also been suggested in several systems.[25−27] However, most of these structures, whether disk-ring structure, oligomer clusters, or 3D multilayer meta-atoms, are generally complex and difficult to fabricate. Besides, these top-down-fabricated structures have larger loss due to more defects, which makes sharp resonances difficult in reality. Therefore, searching for new simple structures that support Fano resonances with a narrow line width and a high quality factor has stimulated continuing efforts. Lisa V. Brown et al. in Naomi J. Halas's group realized Fano resonances based on a very simple system, that is, nanosphere−nanoshell heterodimers, and gave a detailed analysis on the coupling between multiple modes.[28] Quasi-one-dimensional nanostructures, that is, nanorods, nanorice, and nanowires, which can be chemically synthesized and can support tunable plasmon resonant modes in a large range, offer another way to approach the above goal. Recently, nanorod-based simple plasmonic Fano structures have been proposed in several theoretical papers.[29,30] In addition, plasmon-induced transparency (PIT), which appears when perfect interference happens during Fano resonance generation, was reported in self-assembly nanorod systems by Sushmita Biswas et al.[31]

Another phenomenon related to plasmon sensing is the optical activity of plasmonic nanostructures, which is rapidly developing due to its wide applications in biology, chemistry, and medicine.[32−35] It was first observed in chiral structures, such as planar metamaterials,[36] a three-dimensional metamaterial of mutually twisted planar metal patterns,[37] and self-assembled nanoparticles in a chiral complex.[38,39] In 2009, E. Plum et al. reported that optical activity could also be generated

Received: July 7, 2014
Published: September 24, 2014

in achiral structures when they were subjected to obliquely incident light,[33] the so-called "extrinsic optical activity", which offers an alternative method to solve the difficulty of fabricating complex chiral structures.

In this paper, we propose a very simple structure: a silver nanorice heterodimer, in which Fano resonances and strong optical activity coexist. A special hybridization picture in which the hybridized subradiant and super-radiant modes are relatively closer to each other benefits the generation of Fano resonances. Higher-order Fano resonances are observed under oblique incidence. In addition, due to symmetry breaking by oblique illumination, the structure shows strong optical activity in Fano resonant ranges. A further parameter-dependent study shows Fano resonances have an assisting effect on optical activity. To the best of our knowledge, this is the first time that the effect of Fano resonances on optical activity is studied.

SIMULATION METHOD AND EXCITATON MODEL

The finite element method (FEM) (COMSOL Multiphysics) is used to perform our simulations. Our nanorice heterodimer consists of a pair of parallel Ag nanorices with different sizes, as shown in Figure 1, with corresponding geometrical parameters

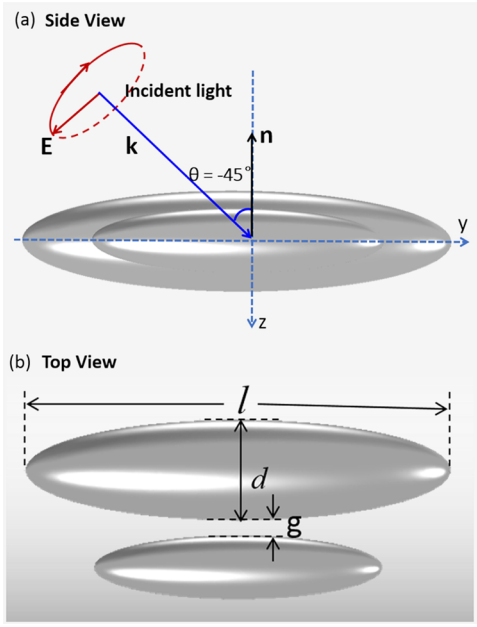

Figure 1. Excitation model of a Ag nanorice heterodimer. (a) Side view: The Ag nanorice dimer locates in the $x-y$ plane, with its normal direction **n** along the negative direction of the z axis. Linearly or circularly polarized light illuminates this structure, with normal incidence (θ = 0°) or oblique incidence (θ = 45° or θ = −45°, depending on the incident wave vector **k** on the right or left side of the normal direction **n** in the $y-z$ plane). (b) Top view of the nanorice dimer. Geometrical parameters are labeled in the structure.

marked in Figure 1b. For convenience, we name each dimer $l_1(d_1)-l_2(d_2)$, where $l_1(d_1)$ is the length (diameter) of the longer rice, and $l_2(d_2)$ is for the shorter one. The permittivity of silver was taken from the experimental data reported by Johnson and Christy.[40] In the simulation, we used a homogeneous surrounding medium with refractive index n = 1.1 as the background. This simple model has been justified to characterize the influence of the glass substrate holding the nanoparticles.[41] The effect of the substrates, which is only moderate, is discussed in the end of the Discussion section. Linearly and circularly polarized light under normal or oblique incidence (refer to Figure 1a) are used to excite this structure, which will be studied in the following. Electromagnetic fields on an imaginary spherical surface with a radius larger than 300 nm enclosing the structure was used to calculate the far-field scattering cross section with the Stratton−Chu formula. The absorption cross section was calculated by integrating the ohmic heating within the Ag heterodimer. The technique of perfectly matched layer was used to minimize the scattering from the boundary. Nonuniform meshes were adopted in the calculation. The largest mesh was set less than 1/12 the wavelength.

RESULTS AND DISCUSSION

Mode Hybridization under Normal Incidence. First we consider normal incidence (θ = 0°) with linearly polarized light. The polarization is along the long axis of the nanorice. Figure 2a-i shows the calculated scattering spectrum of the

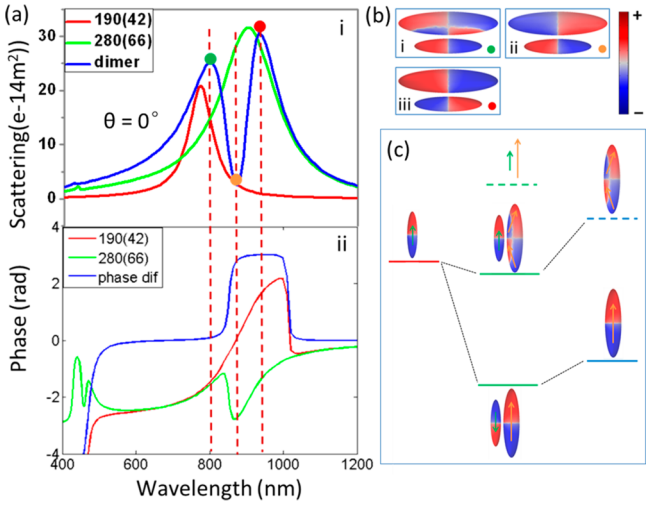

Figure 2. Scattering properties of the dimer 280(66)−190(42) with gap g = 10 nm under normal incidence. (a) Calculated scattering (i) and phase of the electric field (ii) for the heterodimer (blue curves) and individual nanorice composing the dimer (red and green curves). The phase of the electric field is obtained at the nanorice end of the heterodimer. (b) Surface charge distributions for the hybridized plasmon modes marked by colored dots on the scattering spectrum in (a). (c) Energy-level diagram describing the plasmon hybridization in this heterodimer. Underlying dashed lines indicate that corresponding modes cannot be excited directly under this excitation.

heterodimer 280(66)−190(42), as well as the scattering spectra of the two individual nanorices composing it. It can be seen that for these two individual nanorices only dipole modes (red and green curves) are excited. However, when the two nanorices are placed together with a 10 nm gap, two asymmetric peaks with a sharp dip between them distinguish the spectrum. Compared with the resonant positions of the dipole modes of the two individual nanorices, both of the hybridized modes red-shift, which is different from previously reported two-nanoparticle hybridization. In order to identify the hybridized modes, we plot the surface charge distributions corresponding to the two peaks and the dip in the hybridized spectrum, as shown in Figure 2b-i−iii. Obviously, the peak in the longer wavelength is hybridized from dipole modes of the two nanorices, and the charge distribution (Figure 2b-iii) shows this is a subradiant

dx.doi.org/10.1021/ph5002457 | ACS Photonics 2014, 1, 1156−1164

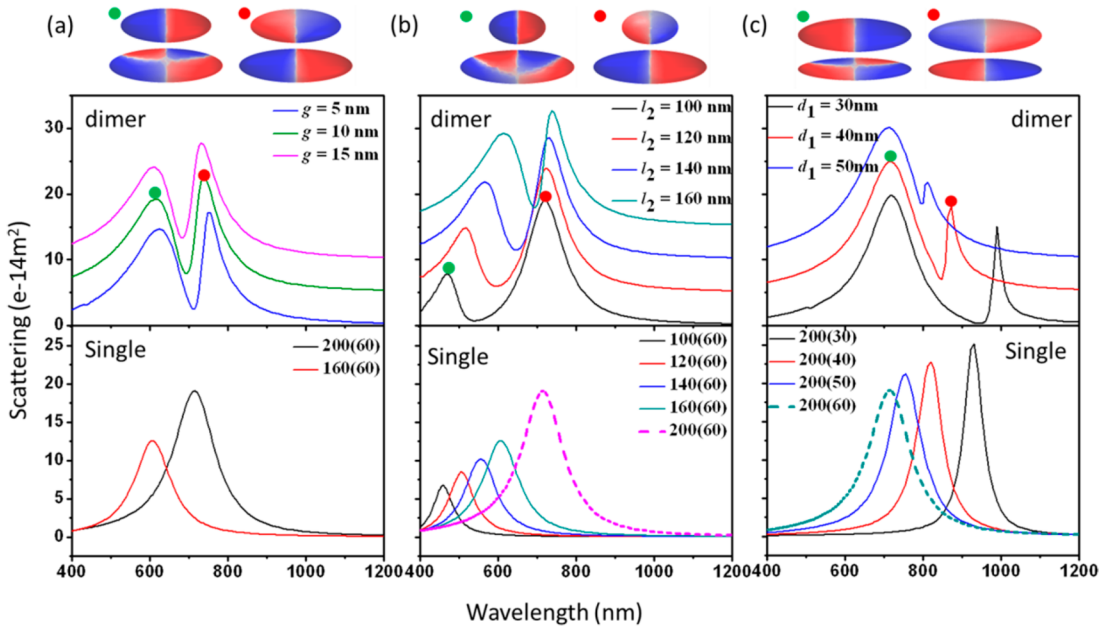

Figure 3. Dependence of Fano interferences on gap (a), nanorice length (b), and nanorice diameter (c). Top: Surface charge distributions of plasmon modes marked by colored dots in the below scattering spectra. Middle: Scattering spectra of (a) two coupled Ag nanorices (200(60) and 160(60)) with different gaps, (b) Ag nanorice heterodimers 200(60)–l_2(60) with different length l_2, and (c) Ag nanorice heterodimers 200(d_1)–200(60) with different d_1. To make a better perspective, every spectrum in this part has an offset greater by 5×10^{-14} m^2 than the one below it. Bottom: Scattering spectra of corresponding single nanorices that compose the above heterodimers. Spectrum in dashed line is for the rice kept unchanged. Gap between the two nanorices is fixed at 10 nm in (b) and (c).

bonding dipole–dipole mode; the peak in the short wavelength is hybridized from the quadruple mode of the longer nanorice and the dipole mode of the shorter nanorice, identified as a bright bonding quadruple–dipole mode (Figure 2b-i). One should notice that under such an excitation usually only higher-order odd modes with more nodes along the long axis of the nanorice can be excited,[42] not a usual quadruple mode. In the situation of a nanorice heterodimer, because of the ellipsoid shape of the nanorice, the quadruple mode is always induced by the other nanorice in the plane normal to the light propagating direction, whose hybridization with the modes of the other nanorice always results in a super-radiant lower energy bonding mode. Thus, it is easier for this super-radiant mode to overlap with the low-energy subradiant mode, benefiting the generation of Fano resonance. The dipole–dipole antibonding mode of the heterodimer cannot be excited in such a configuration because of the induced charge. For the dip in the scattering spectrum, here it shows the same charge distribution with the longer wavelength peak, but with lower charge density and a different phase. The above analysis indicates the overlap and interference between the bright dipole–quadruple mode and the subradiant bonding dipole–dipole mode induce the asymmetric Fano profile in the spectrum. Figure 2a-ii shows the wavelength dependence of the phase of the electric field at the nanorice ends of the heterodimer and the phase difference between them. The phase difference is π between the dip and the peak of the longer wavelength and zero between the dip and the peak of the short wavelength, which is in agreement with the above analysis of the modes. The energy-level diagram shown in Figure 2c describes the hybridization of the plasmon modes supported by this Ag nanorice heterodimer system.

To further investigate the phenomenon, the dependence of Fano resonance on several parameters of the system is studied as well, as shown in Figure 3. Figure 3a shows spectra of heterodimers of 200(60)–160(60) with different gap distance g. Compared with the dipole modes of individual nanorices shown in the bottom panel, the two hybridized modes supported by each heterodimer both red-shift and show an asymmetric Fano profile, which is similar to Figure 2. With the decrease of the distance between two nanorices, the interaction becomes stronger, which makes the two hybridized bonding modes red-shift. Yet even with the large distance of g = 15 nm, the Fano profile of the spectrum is still distinctive. The charge distribution shown in the top panel indicates that the Fano resonance here follows the same mechanism as in Figure 2. Note that the intensity of the dip between the two peaks in the spectrum can decrease to almost zero, which means a nearly perfect transparency can be realized in this system. In fact, plasmon-induced transparency has been reported in a similar nanorod system recently.[31] The relative size of the two nanorices has a significant effect on the Fano interference. Figure 3b shows spectra of heterodimers with the same diameters and gap distance, but with a changing length of the shorter nanorice. When the length difference between the two nanorices becomes very large, such as in the case of l_1 = 200 nm and l_2 = 100 nm, the line shape of the hybridized spectrum becomes more symmetric. From the charge distribution shown in the top panel, it can be seen that the longer wavelength mode is not dark enough since the longer nanorice has a dominant dipole moment due to its higher charge density and larger size, which makes the whole structure exhibit a mode more like the mode of the longer nanorice. Similarly, the shorter wavelength mode is not bright enough since the net moment along the long axis is small. More importantly, the relatively large resonant energy difference of the two modes makes little overlap of the two peaks, which results in weak interference insufficient for a distinctive Fano profile. As the length of the small nanorice becomes longer, the resonant

dx.doi.org/10.1021/ph5002457 | ACS Photonics 2014, 1, 1156–1164

energy difference becomes smaller, so that the overlap of the two modes is larger. As a result, the asymmetric Fano profile becomes more distinctive. It is interesting to see that for heterodimers composed of two nanorices with the same length but a small difference in diameter, a distinctive (actually much sharper) Fano resonance can also be excited, as shown in Figure 3c. This further demonstrates that the special shape of the nanorice makes their coupling different from those in other nanoparticle systems. The reason for the particular behavior of plasmon hybridization is that for two parallel-arranged nanorices here their ends are relatively far from each other, while for the middle region between the two nanorices, the strong coupling will induce the quadruple mode of the lower energy nanorice, the same as above. But as the length of the nanorices are the same, the subradiant mode will be darker, and the two hybridized resonant peaks are closer, which subsequently produces a much sharper Fano profile.

Higher-Order Fano Resonances under Oblique Incidence. When the nanorice dimer is illuminated obliquely, higher-order modes could be excited because of a retardation effect, as shown in Figure 4a. The hybridization and

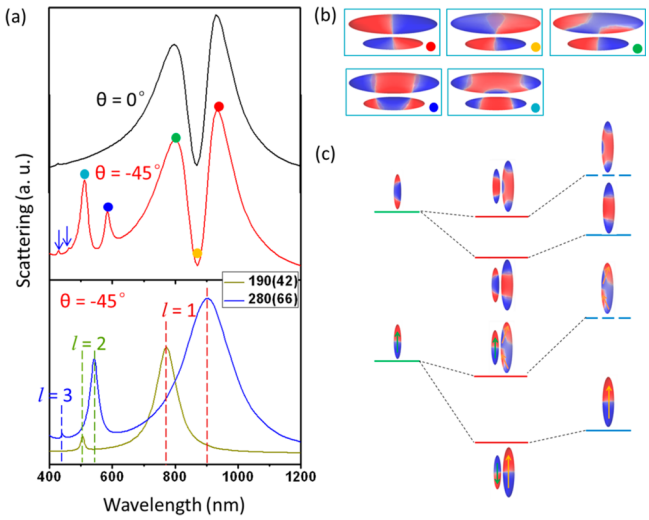

Figure 4. Scattering properties of the same heterodimer as the one in Figure 2 under oblique incidence. (a) Top: Calculated scattering spectra when $\theta = 0°$ (black, normal incidence, given here for comparing with the oblique incidence), $\theta = -45°$ (red, oblique incidence). Bottom: Scattering spectra of individual nanorices when $\theta = -45°$. (b) Surface charge distributions for hybridized plasmon modes (marked by colored dots in (a)) under oblique incidence. (c) Energy-level diagram describing the plasmon hybridization of the Ag heterodimer under oblique excitation.

interference of these modes can yield higher-order Fano resonances. For example, when the same nanorice heterodimer as the one in Figure 2 is illuminated with an incident angle of $\theta = -45°$ (Figure 1a), and the polarization is in the incident plane, six peaks appear in the scattering spectrum (Figure 4a, red curve). Here we focus only on the four distinctive peaks marked by colored dots. For the two peaks in the long-wavelength range, they are the same as the previous ones in Figure 2 (i.e., Figure 4a, black curve). Charge distributions shown in Figure 4b can verify this point. For the other two peaks in the short-wavelength range, we first plot the surface charge distribution of each peak (Figure 4b, marked by blue and cyan dots). It can be seen that the blue dot peak is the bonding mode of $l = 2$ modes of the two nanorices, while the cyan dot peak seems like an antibonding mode of the $l = 2$ modes of the nanorices; however, the curved shape of the smaller nanorice induces a higher-order mode on the longer nanorice, whose hybridization with the smaller nanorice generates eventually a bonding mode and lowers the energy. Comparing the red curve of the heterodimer in the top panel in Figure 4a with the blue and green curves of individual nanorices in the lower panel in Figure 4a, one can see that both peaks here red-shift. The interference of the two hybridized modes then brings out an asymmetric Fano profile, being similar to the hybridization case of dipole (or $l = 1$) modes. Compared with the normal incidence, the oblique incidence here causes retardation along the long axis of the nanorice, which induces higher-order modes of the nanorice. The other two higher-order modes ($l = 3$) indicated with blue arrows in Figure 4a have very similar situations in mode hybridization.

The Fano resonance formed by the interference here is different from most previously published works. Structures studied before usually have substructures to support a separate bright mode and a separate dark mode individually. For example, in the previous dolmen-style strip, the bright (dark) mode was excited on the vertical strip, while the two parallel strips gave the excitation of the dark (bright) mode.[43] Some core−shell structures have similar hybridization.[44,45] Besides, Fano resonances supported by the Ag heterodimers are very sensitive to the surrounding environments (Figure S1 in the Supporting Information). The energy shift for the higher-order mode reaches 1.76 eV per refractive index unit (RIU). Especially, when the two nanorices have the same length but a small difference in diameter, the low-order subradiant mode becomes very narrow, and a much higher figure of merit (FOM) of ∼26 can be obtained. This is different from the normal case, in which a lower-order mode usually has a low FOM. All the results suggest that a Ag nanorice heterodimer is a highly suitable substrate for localized surface plasmon resonance (LSPR) sensing.

Optical Activity Generated under Oblique Incidence. Although the nanorice heterodimer under normal incidence is a 2D structure without any chiral characteristic, when excited obliquely along the long axis of the nanorice, this structure meets three conditions that will lead to chirality even though the material is nonchiral: (1) no inversion center (met by the structure itself); (2) no reflection symmetry in the plane perpendicular to the propagation direction; (3) no inversion or mirror rotation axis along the propagation direction.[33,46] The last two conditions are met by oblique incidence and different sizes of the two nanorices. Different tilted angles will cause different chiral effects.[47,48] Here we study only situations where the angle is −45° and 45°. As Figure 5a and the red curve in Figure 5b show, when the structure is illuminated at $\theta = -45°$ (the same as in Figure 4), but with a circularly polarized light, the extinction spectra show a remarkable difference between RCP and LCP excitation, especially in the vicinity of the four Fano resonance peaks, with the difference reaching a maximum at some higher-order mode. It can also be seen that the extinction cross section of the subradiant modes (both low- and high-order modes) is larger under RCP light excitation, while the two bright modes show stronger extinction with LCP. An interesting point is that this structure performs almost as a purely right- or left-handed system at the higher-order subradiant mode (marked as "iii" in Figure 5a) since this mode nearly disappears under illumination of the opposite

dx.doi.org/10.1021/ph5002457 | ACS Photonics 2014, 1, 1156−1164

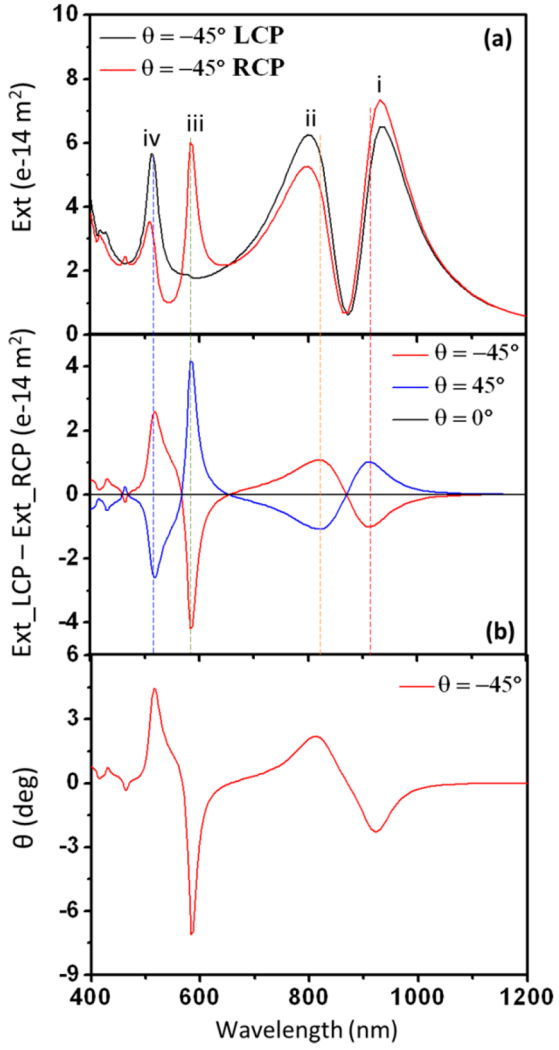

Figure 5. Optical activity of the Ag nanorice heterodimer generated under oblique incidence. (a) Left and right circularly polarized (LCP and RCP) light obliquely ($\theta = -45°$) excited extinction spectra of a nanorice heterodimer with the same size as in Figure 4. (b) Difference of extinction cross sections between LCP and RCP excitations when $\theta = -45°$ (red), $\theta = 45°$ (blue), and $\theta = 0°$ (black). (c) Estimated CD in degrees with a 500 nm × 250 nm unit cell in a 1 cm × 1 cm sample area when $\theta = -45°$.

handedness of light (also refer to Figure S2 in the Supporting Information). In the simulated spectra, the optical activity (i.e., CD) in units of M^{-1} cm^{-1} for one heterodimer could be estimated by

$$\Delta\varepsilon_{mol} \propto \sigma_L - \sigma_R$$

where σ_L and σ_R are the extinction cross sections of the structure under LCP and RCP excitation. As shown in Figure 5a and b, all modes show strong CD, including subradiant modes. If we assume that each unit cell (i.e., one heterodimer) occupies a 500 nm × 250 nm area, then in a 1 cm × 1 cm sample, we could estimate CD in degrees as shown in Figure 5c and the transmission (Figure S3 in the Supporting Information).

The microscopic origin of the optical activity in the extrinsically chiral nanorice heterodimer can be understood by comparing with conventional optical activity of a chiral molecule, where the effect comes from interaction of the electric and magnetic responses. The circular dichroism signal in units of M^{-1} cm^{-1} is estimated by

$$\Delta\varepsilon_{mol} \propto \mathrm{Im}[\vec{d}\cdot\vec{m}]$$

where $\vec{d}$ and $\vec{m}$ are the electric and magnetic dipole moments of the molecule.[49] Here in the nanorice heterodimer, the surface current distributions of different modes can be represented as the sum of a straight current along the nanorice surface and current loops at the gap, which will induce corresponding electric and magnetic dipole moments, respectively, as shown in Figure 6a. The induced electric and

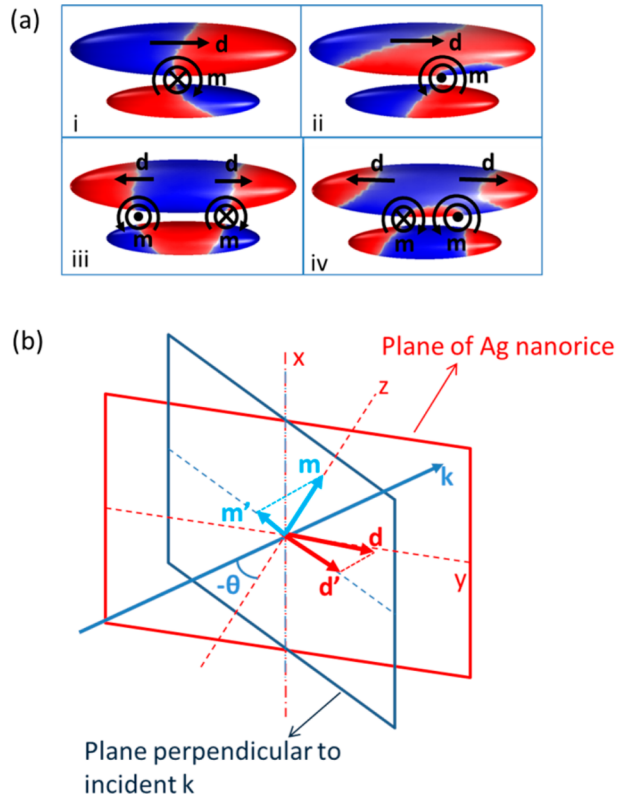

Figure 6. Generation mechanism of the optical activity. (a) Surface charge distributions for the four modes excited by RCP light and marked by i, ii, iii, and iv in Figure 5a. Induced equivalent electric dipole and magnetic dipole moments are marked as "d" and "m". (b) Schematic of optical activity generation mechanism for the lowest mode (i). The projections of magnetic dipole moment m′ and the electric dipole moment d′ in the plane perpendicular to the incident light can reduce LCP light but increase RCP light, generating the optical activity.

magnetic dipole moments have a similar response to the incident electromagnetic field to those in chiral molecules. When the structure is illuminated by tilted light, the induced electric dipole moment d and magnetic dipole moment m both have projections in the plane perpendicular to the incident wave vector. Figure 6b shows the case for the lowest mode, with projections of dipole moments marked as d' and m'. The coplanar electric and magnetic dipole moments (with parallel components) will emit electromagnetic waves with orthogonal polarizations in the direction of wave propagation, which will rotate the polarization of incident light, and then generate the optical activity. Thus, this artificial "metamolecule" has extrinsic optical activity because of the symmetry breaking induced by

dx.doi.org/10.1021/ph5002457 | ACS Photonics 2014, 1, 1156−1164

oblique illumination. Other modes having different projections that make different chirality can be analyzed analogously. Higher-order modes have more than one pair of coplanar electric and magnetic dipole moments, whose effect on chirality will be discussed later in the Discussion section.

It can be deduced from the above analysis that the optical activity should disappear under normal incidence ($\theta = 0°$) since the induced electric dipole and magnetic dipole moments are perpendicular to each other. This is verified by the simulation result shown by the black curve in Figure 5b. Furthermore, as expected in the analytical model, the sign of optical activity, which is determined by the mutual phase difference between the electric and magnetic responses, should depend on the sign of the tilting angle (here represented by the sign of θ). Figure 5b exactly verifies this point: the optical activity is reversed when the incident angle is changed from $\theta = -45°$ to $\theta = 45°$.

It is worth mentioning that all modes in Figure 5 show strong CD, including subradiant plasmonic modes. Originally, these subradiant modes are difficult to excite because of their weak moments, despite their potential to exhibit chiral behavior. However, in the Fano resonance situation, the energy transfer between the super-radiant mode and the subradiant mode can assist, even enhance, the chirality of subradiant modes, making them observable. In order to reveal this effect, the dependence of optical activity on several parameters is studied in the following.

Figure 7 shows the effect of changing gap distance on the optical activity. For a heterodimer 200(60)−100(30), when the gap between the two coupled nanoparticles is decreased from 30 nm to 10 nm, the extinction cross sections as a whole do not change much; however, the differences of extinction cross sections between LCP and RCP excitations (Figure 7b) for the smaller gap case are about 2 times larger than that for the larger gap, which indicates that the smaller gap and thus stronger Fano interference will generate stronger optical activity.

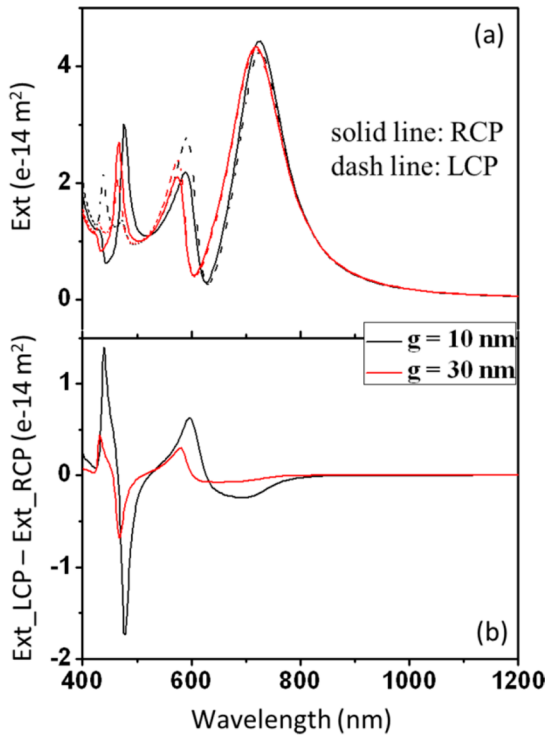

Figure 7. Optical activity with different gaps between the two nanorices. (a) Extinction of the Ag nanorice dimer 200(60)−100(30) with gap g = 10 nm (black) and g = 30 nm (red) under LCP and RCP excitation. (b) Difference of extinction between LCP and RCP.

The length and diameter of nanorices are also tuned. As shown in Figure 8a, when the length l_1 of the big nanorice is reduced from 180 nm to 120 nm, while the small nanorice (100(30)) remains unchanged, the Fano profile of the extinction spectrum becomes more distinctive due to the increasing energy overlap of the two nanoparticles. Although the extinction cross section of the lowest energy mode decreases significantly in this process, the extinction difference (Figure 8b) is almost unchanged, or even increases slightly. When the two nanorices have the same length, the Fano profile is very sharp, and the subradiant mode is very dark, which is only a small peak on the background of the bright mode peak. However, the extinction difference is very large (see Figure S4 in the Supporting Information). This from another perspective means the Fano resonance has an "assisting effect" on optical activity. The case for higher-order modes is complex because several modes hybridized together. Studies on changing diameters of nanorices in Figure 8c and d also show a similar assisting effect. When the diameter of the larger nanorice increases from 40 nm to 70 nm, with other parameters unchanged, plasmonic modes of this nanorice blue-shift and have a larger overlap with the smaller nanorice, resulting in stronger Fano interference. As expected, the extinction difference (Figure 8d) gradually increases in this process, although the extinction cross section decreases.

From Figure 5 one can also find that the two chiral peaks of the lower-order modes in Figure 5b locate at wavelengths between the corresponding extinction peaks and dip in Figure 5a (similar phenomena also appear in Figures 6−8). These wavelengths may correspond to the primitive modes before Fano interference. It is well known that, in the Fano resonance, the π phase difference between the two original resonant peaks results in the Fano dip and peaks because of the interference. So the original resonant modes usually locate between the resultant Fano dip and corresponding peaks. Yet the positions of original modes can be indicated by corresponding absorption peaks. Figure 9 shows extinction, absorption, and extinction difference of two heterodimers. It can be seen clearly that the two lower-order chiral peaks (actually it is the same as higher-order modes) in Figure 9c appear at positions of the corresponding absorption peaks (Figure 9b), verifying our supposition. More evidence is given in Figure S4 in the Supporting Information.

DISCUSSION

In the above, we refer to the strong CD manifested by subradiant modes as a "Fano-assisted CD" effect and investigate it with different parameters. Here we give a further description and discussion on it. When the super-radiant and subradiant modes are far from each other, this energy transfer is insufficient, and thus the CD peak is still at the position of the subradiant peak. It can still be observed mainly because the subradiant mode is not so dark, while when the resonant energies of the two nanorices are closer, the subradiant mode becomes very dark and cannot be excited directly, though the system still has strong chirality. However, in this case of stronger Fano resonance, because the subradiant mode is close to the super-radiant mode, the interaction of the two modes is manifested not only as interference when they emit in far field but also as an energy transfer between them, which efficiently

dx.doi.org/10.1021/ph5002457 | ACS Photonics 2014, 1, 1156−1164

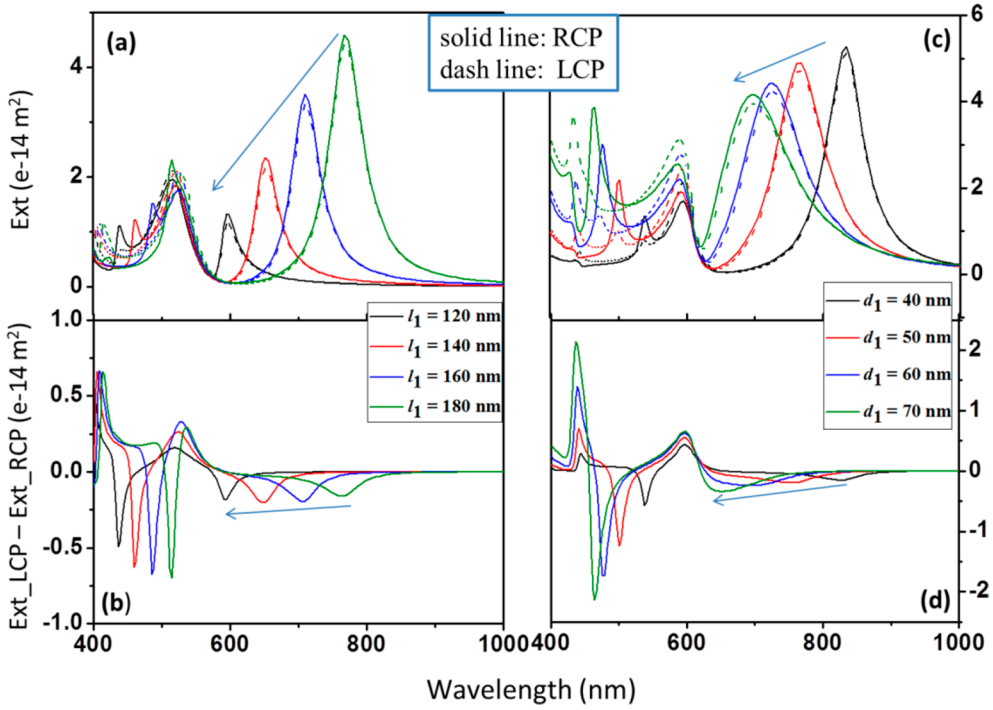

Figure 8. Influence of length (a, b) and diameter (c, d) of nanorices on optical activity. Extinction and extinction difference for heterdimers (a, b) $l_1(40)-100(40)$ and (c, d) $200(d_1)-100(30)$. The gap is fixed at g = 10 nm. The arrows indicate the variation trend.

excites the dark mode. This dark mode is formed by two antiparallel dipoles, here whose response to the incident light behaves in the same way as a combination of a magnetic dipole and an electric dipole. A very typical example in which the two nanorices have the same length and very close diameters is given in Figure S4 in the Supporting Information. The subradiant mode of this configuration is very dark, as the two excited antiparallel dipoles have a very close strength, and the peak intensity of the subradiant mode is also very small if the strong background of the super-radiant mode is taken away. However, the extinction difference of this mode reaches 0.6 × 10^{-14} m^2, which is even bigger than the other cases.

Another interesting thing mentioned above is that higher-order modes manifest much stronger CD than the first-order modes, and furthermore, in many cases, the "metamolecule" behaves like a totally right (or left) handed structure at these modes (Figures 5a, 8a,c, 9a, and S2). From these figures one can see that when the structures are excited with LCP (or RCP) light, the subradiant peaks are very weak or almost disappear (the black line in Figure 5a, the green dashed line in Figure 8c, the red dashed line in Figure 9a, and the green line in Figure S2). From surface charge distributions of Figure 6a-iii and -iv, we know that there is more than one pair of interacting equivalent electric and magnetic dipoles for these modes, and they have a synergetic effect on the chirality of the same mode because the dot production of each pair of dipole moments has the same sign. Note that due to phase retardation, the electric or magnetic dipoles that appear to be antiparallel on the surface cannot just simply cancel each other; instead, they have a sum effect. The spectra with the almost vanished LCP (RCP) higher-order peaks mean that the electric and magnetic dipoles can interact so strongly that the corresponding handedness is fully prohibited. This shows that a totally right (left)-handed plasmonic structure can be realized, which may have potential applications in related fields.

Although all the simulations are performed with the structure embedded in homogeneous medium, the above conclusions can be extended to the case of Ag heterdomers on a glass substrate (Figure S5 in the Supporting Information). Extinctive Fano resonances and strong optical activity are also observed. However, there are some slight differences between the two cases. Compared with the uniform case, the positions of all resonant modes have a slight blue-shift, which is probably because the gap between the two nanorices is larger than that of the uniform case, as shown in Figure S5c, and the position shift also results in a smaller electric field component in the line connecting the center of the two nanorices. Besides, the CD signal is weaker than that of the uniform case, which is probably because the substrate changes the symmetry of the system, and the weaker coupling is induced by the larger gap. However, the CD signal is still much larger than most of the previously reported results.

CONCLUSION

In conclusion, plasmonic properties of parallel-arranged nanorice heterodimers under different illumination are theoretically investigated. Due to the special ellipsoid shape, this structure manifests some novel properties. Distinctive multipolar Fano resonances are obtained, with near zero intensity in the dip position of the extinction spectrum, which makes them good candidates for PIT and ultrasensitive sensing. More interestingly, due to symmetry breaking by oblique illumination, the structure shows strong optical activity in the Fano resonance ranges. A chiral molecule model has been proposed to understand the generation of chirality. Investigations on length, thickness, and gap dependence indicate that Fano resonances have an "assisting effect" on CD, which is ascribed to the energy transfer from the super-radiant modes to the subradiant modes in the Fano resonance. At some high-order modes, strong interaction makes the structure exhibit

dx.doi.org/10.1021/ph5002457 | ACS Photonics 2014, 1, 1156−1164

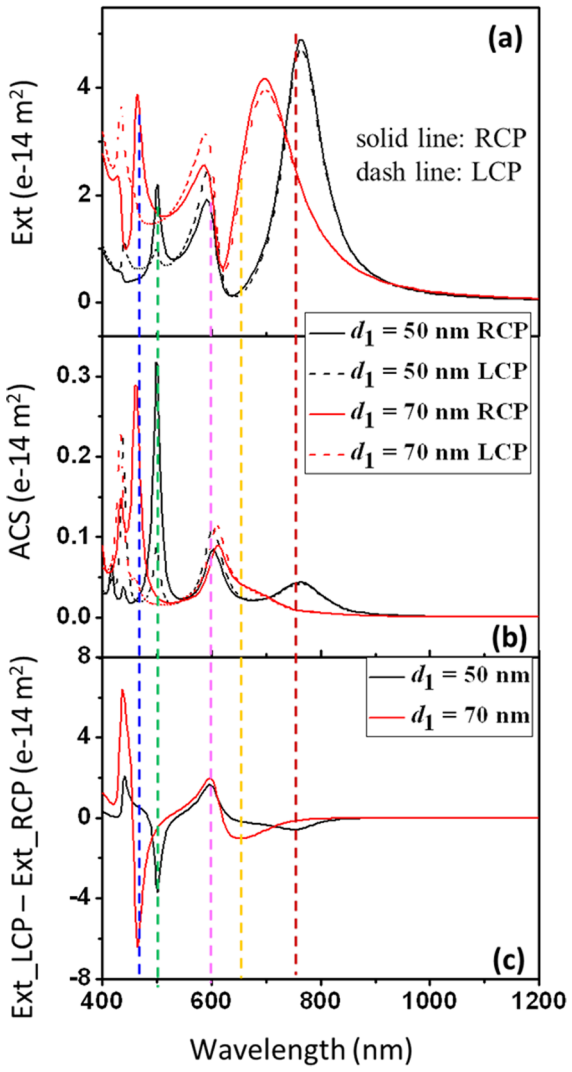

Figure 9. Extinction (a), absorption cross section (ACS) (b), and extinction difference (c) for heterodimers 200(d_1)−100(30) with g = 10 nm.

even totally right (left) handedness. The high CD effect may have promising applications in related fields.

■ ASSOCIATED CONTENT

Supporting Information

Figure S1, Sensitivity of Fano resonances to the environmental refractive index. Figure S2, Extinction spectra of the same nanorice heterodimer as that in Figure 5 when θ = 0° and θ = 45°. Figure S3, Estimated transmission spectra of the same nanorice heterodimer as that in Figure 5. Figure S4, Another evidence mentioned in the text. Figure S5, Effects of substrate on optical properties of Ag nanorice heterodimers. This material is available free of charge via the Internet at http://pubs.acs.org.

■ AUTHOR INFORMATION

Corresponding Authors

*E-mail: yurui.fang@chalmers.se.
*E-mail: blzhang@ntu.edu.sg.

Notes

The authors declare no competing financial interest.

■ ACKNOWLEDGMENTS

The authors thank Li Chen for helpful discussions. This work was sponsored by Nanyang Technological University under a Start-Up Grant and a NAP Grant, and Singapore Ministry of Education under Grant No. Tier 1 RG27/12 and No. MOE2011-T3-1-005.

■ REFERENCES

(1) Halas, N. J.; Lal, S.; Chang, W. S.; Link, S.; Nordlander, P. Plasmons in strongly coupled metallic nanostructures. *Chem. Rev.* **2011**, *111*, 3913−3961.
(2) Moskovits, M. Surface-enhanced Raman spectroscopy: a brief perspective. *Top. Appl. Phys.* **2006**, *103*, 1−17.
(3) Xu, H. X.; Bjerneld, E. J.; Käll, M.; Börjesson, L. Spectroscopy of single hemoglobin molecules by surface enhanced Raman scattering. *Phys. Rev. Lett.* **1999**, *83*, 4357−4360.
(4) Kneipp, K.; Wang, Y.; Kneipp, H.; Perelman, L. T.; Itzkan, I.; Dasari, R.; Feld, M. S. Single molecule detection using surface-enhanced Raman scattering (SERS). *Phys. Rev. Lett.* **1997**, *78*, 1667−1670.
(5) Kall, M.; Xu, H. X.; Johansson, P. Field enhancement and molecular response in surface-enhanced Raman scattering and fluorescence spectroscopy. *J. Raman Spectrosc.* **2005**, *36*, 510−514.
(6) Fang, Y. R.; Li, Z. P.; Huang, Y. Z.; Zhang, S. P.; Nordlander, P.; Halas, N. J.; Xu, H. X. Branched silver nanowires as controllable plasmon routers. *Nano Lett.* **2010**, *10*, 1950−1954.
(7) Zhang, S. P.; Wei, H.; Bao, K.; Hakanson, U.; Halas, N. J.; Nordlander, P.; Xu, H. X. Chiral surface plasmon polaritons on metallic nanowires. *Phys. Rev. Lett.* **2011**, *107*, 096801.
(8) Dickson, R. M.; Lyon, L. A. Unidirectional plasmon propagation in metallic nanowires. *J. Phys. Chem. B* **2000**, *104*, 6095−6098.
(9) Muhlschlegel, P.; Eisler, H. J.; Martin, O. J. F.; Hecht, B.; Pohl, D. W. Resonant optical antennas. *Science* **2005**, *308*, 1607−1609.
(10) Wei, H.; Li, Z. P.; Tian, X. R.; Wang, Z. X.; Cong, F. Z.; Liu, N.; Zhang, S. P.; Nordlander, P.; Halas, N. J.; Xu, H. X. Quantum dot-based local field imaging reveals plasmon-based interferometric logic in silver nanowire networks. *Nano Lett.* **2011**, *11*, 471−475.
(11) Linic, S.; Christopher, P.; Ingram, D. B. Plasmonic-metal nanostructures for efficient conversion of solar to chemical energy. *Nat. Mater.* **2011**, *10*, 911−921.
(12) Prodan, E.; Radloff, C.; Halas, N. J.; Nordlander, P. A hybridization model for the plasmon response of complex nanostructures. *Science* **2003**, *302*, 419−422.
(13) Fan, J. A.; Wu, C. H.; Bao, K.; Bao, J. M.; Bardhan, R.; Halas, N. J.; Manoharan, V. N.; Nordlander, P.; Shvets, G.; Capasso, F. Self-assembled plasmonic nanoparticle clusters. *Science* **2010**, *328*, 1135−1138.
(14) Jain, P. K.; Huang, W. Y.; El-Sayed, M. A. On the universal scaling behavior of the distance decay of plasmon coupling in metal nanoparticle pairs: a plasmon ruler equation. *Nano Lett.* **2007**, *7*, 2080−2088.
(15) Liu, N.; Hentschel, M.; Weiss, T.; Alivisatos, A. P.; Giessen, H. Three-dimensional plasmon rulers. *Science* **2011**, *332*, 1407−1410.
(16) Kuzyk, A.; Schreiber, R.; Fan, Z. Y.; Pardatscher, G.; Roller, E. M.; Hogele, A.; Simmel, F. C.; Govorov, A. O.; Liedl, T. DNA-based self-assembly of chiral plasmonic nanostructures with tailored optical response. *Nature* **2012**, *483*, 311−314.
(17) Willets, K. A.; Van Duyne, R. P. Localized surface plasmon resonance spectroscopy and sensing. *Annu. Rev. Phys. Chem.* **2007**, *58*, 267−297.
(18) Szunerits, S.; Boukherroub, R. Sensing using localised surface plasmon resonance sensors. *Chem. Commun.* **2012**, *48*, 8999−9010.
(19) Luk'yanchuk, B.; Zheludev, N. I.; Maier, S. A.; Halas, N. J.; Nordlander, P.; Giessen, H.; Chong, C. T. The Fano resonance in plasmonic nanostructures and metamaterials. *Nat. Mater.* **2010**, *9*, 707−715.
(20) Miroshnichenko, A. E.; Flach, S.; Kivshar, Y. S. Fano resonances in nanoscale structures. *Rev. Mod. Phys.* **2010**, *82*, 2257−2298.

(21) Zhang, S. P.; Bao, K.; Halas, N. J.; Xu, H. X.; Nordlander, P. Substrate-induced fano resonances of a plasmonic: nanocube: a route to increased-sensitivity localized surface plasmon resonance sensors revealed. *Nano Lett.* **2011**, *11*, 1657−1663.
(22) Ye, J.; Wen, F. F.; Sobhani, H.; Lassiter, J. B.; Van Dorpe, P.; Nordlander, P.; Halas, N. J. Plasmonic nanoclusters: near field properties of the Fano resonance interrogated with SERS. *Nano Lett.* **2012**, *12*, 1660−1667.
(23) Zhang, Y.; Wen, F.; Zhen, Y. R.; Nordlander, P.; Halas, N. J. Coherent Fano resonances in a plasmonic nanocluster enhance optical four-wave mixing. *Proc. Natl. Acad. Sci. U.S.A.* **2013**, *110*, 9215−9219.
(24) Metzger, B.; Schumacher, T.; Hentschel, M.; Lippitz, M.; Giessen, H. Third harmonic mechanism in complex plasmonic Fano structures. *ACS Photonics* **2014**, *1*, 2330−4022.
(25) Fu, Y. H.; Zhang, J. B.; Yu, Y. F.; Luk'yanchuk, B. Generating and manipulating higher order Fano resonances in dual-disk ring plasmonic nanostructures. *ACS Nano* **2012**, *6*, 5130−5137.
(26) Dregely, D.; Hentschel, M.; Giessen, H. Excitation and tuning of higher-order Fano resonances in plasmonic oligomer clusters. *ACS Nano* **2011**, *5*, 8202−8211.
(27) Artar, A.; Yanik, A. A.; Altug, H. Multispectral plasmon induced transparency in coupled meta-atoms. *Nano Lett.* **2011**, *11*, 1685−1689.
(28) Brown, L. V.; Sobhani, H.; Lassiter, J. B.; Nordlander, P.; Halas, N. J. Heterodimers: plasmonic properties of mismatched nanoparticle pairs. *ACS Nano* **2010**, *4*, 819−832.
(29) Yang, Z. J.; Zhang, Z. S.; Zhang, W.; Hao, Z. H.; Wang, Q. Q. Twinned Fano interferences induced by hybridized plasmons in Au-Ag nanorod heterodimers. *Appl. Phys. Lett.* **2010**, *96*, 131113.
(30) Yang, Z. J.; Zhang, Z. S.; Zhang, L. H.; Li, Q. Q.; Hao, Z. H.; Wang, Q. Q. Fano resonances in dipole-quadrupole plasmon coupling nanorod dimers. *Opt. Lett.* **2011**, *36*, 1542−1544.
(31) Biswas, S.; Duan, J. S.; Nepal, D.; Park, K.; Pachter, R.; Vaia, R. A. Plasmon-induced transparency in the visible region via self-assembled gold nanorod heterodimers. *Nano Lett.* **2013**, *13*, 6287−6291.
(32) Gautier, C.; Burgi, T. Chiral gold nanoparticles. *Chem. Phys. Chem.* **2009**, *10*, 483−492.
(33) Plum, E.; Liu, X. X.; Fedotov, V. A.; Chen, Y.; Tsai, D. P.; Zheludev, N. I. Metamaterials: optical activity without chirality. *Phys. Rev. Lett.* **2009**, *102*, 113902.
(34) Berova, N.; Di Bari, L.; Pescitelli, G. Application of electronic circular dichroism in configurational and conformational analysis of organic compounds. *Chem. Soc. Rev.* **2007**, *36*, 914−931.
(35) Schäferling, M.; Yin, X.; Engheta, N.; Giessen, H. Helical plasmonic nanostructures as prototypical chiral near-field sources. *ACS Photonics* **2014**, *1*, 530−537.
(36) Gao, W. S.; Ng, C. Y.; Leung, H. M.; Li, Y. H.; Chen, H.; Tam, W. Y. Circular dichroism in single-layered gold sawtooth gratings. *J. Opt. Soc. Am. B* **2012**, *29*, 3021−3026.
(37) Plum, E.; Zhou, J.; Dong, J.; Fedotov, V. A.; Koschny, T.; Soukoulis, C. M.; Zheludev, N. I. Metamaterial with negative index due to chirality. *Phys. Rev. B* **2009**, *79*, 035407.
(38) Fan, Z. Y.; Govorov, A. O. Plasmonic circular dichroism of chiral metal nanoparticle assemblies. *Nano Lett.* **2010**, *10*, 2580−2587.
(39) Auguie, B.; Alonso-Gomez, J. L.; Guerrero-Martinez, A.; Liz-Marzan, L. M. Fingers crossed: optical activity of a chiral dimer of plasmonic nanorods. *J. Phys. Chem. Lett.* **2011**, *2*, 846−851.
(40) Johnson, P. B.; Christy, R. W. Optical constants of the noble metals. *Phys. Rev. B* **1972**, *6*, 4370−4379.
(41) Habteyes, T. G.; Dhuey, S.; Cabrini, S.; Schuck, P. J.; Leone, S. R. Theta-shaped plasmonic nanostructures: bringing "dark" multipole plasmon resonances into action via conductive coupling. *Nano Lett.* **2011**, *11*, 1819−1825.
(42) Wei, H.; Reyes-Coronado, A.; Nordlander, P.; Aizpurua, J.; Xu, H. X. Multipolar plasmon resonances in individual Ag nanorice. *ACS Nano* **2010**, *4*, 2649−2654.
(43) Verellen, N.; Sonnefraud, Y.; Sobhani, H.; Hao, F.; Moshchalkov, V. V.; Van Dorpe, P.; Nordlander, P.; Maier, S. A. Fano resonances in individual coherent plasmonic nanocavities. *Nano Lett.* **2009**, *9*, 1663−1667.
(44) Mukherjee, S.; Sobhani, H.; Lassiter, J. B.; Bardhan, R.; Nordlander, P.; Halas, N. J. Fanoshells: nanoparticles with built-in Fano resonances. *Nano Lett.* **2010**, *10*, 2694−2701.
(45) Hao, F.; Sonnefraud, Y.; Van Dorpe, P.; Maier, S. A.; Halas, N. J.; Nordlander, P. Symmetry breaking in plasmonic nanocavities: subradiant LSPR sensing and a tunable Fano resonance. *Nano Lett.* **2008**, *8*, 3983−3988.
(46) Feng, C.; Wang, Z. B.; Lee, S.; Jiao, J.; Li, L. Giant circular dichroism in extrinsic chiral metamaterials excited by off-normal incident laser beams. *Opt. Commun.* **2012**, *285*, 2750−2754.
(47) Lee, S.; Wang, Z. B.; Feng, C.; Jiao, J.; Khan, A.; Li, L. Circular dichroism in planar extrinsic chirality metamaterial at oblique incident beam. *Opt. Commun.* **2013**, *309*, 201−204.
(48) Kruk, S. S.; Decker, M.; Helgert, C.; Staude, I.; Menzel, C.; Powell, D. A.; Etrich, C.; Rockstuhl, C.; Pertsch, T.; Neshev, D. N.; Kivshar, Y. S. Symmetry Properties of Metamaterials at Oblique Incidence. *7th International Congress on Advanced Electromagnetic Materials in Microwaves and Optics − Metamaterials 2013*; IEEE, 2013; pp 205−207.
(49) Barron, L. D. *Molecular Light Scattering and Optical Activity*, 2nd ed.; Cambridge University Press: Cambridge, 2004.